Journal of Photochemistry and Photobiology A: Chemistry 204 (2009) 115–121

Contents lists available at ScienceDirect

Journal of Photochemistry and Photobiology A: Chemistry

journal homepage: www.elsevier.com/locate/jphotochem

A novel microwave photochemical reactor for the oxidative decomposition of Acid Orange 7 azo dye by MW/UV/H_2O_2 process

Carlo Ferrari*, Iginio Longo, Elpidio Tombari, Emilia Bramanti

Institute for Chemical and Physical Processes, I.P.C.F., CNR Research Area of Pisa 1, G. Moruzzi St., 56124 Pisa, Italy

ARTICLE INFO

Article history:
Received 30 January 2009
Received in revised form 19 February 2009
Accepted 3 March 2009
Available online 17 March 2009

Keywords:
Microwave photoreactor
Microwave electrodeless lamp
Hydrogen peroxide
Acid Orange 7
Kinetics

ABSTRACT

The characteristic features of a novel microwave and UV photoreactor, useful for microwave assisted photochemical processes, are presented by examining the results obtained in the photo decoloration of Acid Orange 7 in an aqueous hydrogen peroxide solution. The advantages over other experimental procedures, like reduced consumption of chemicals, energy saving and simpler setup are highlighted. The method enables to activate a chemical reaction with microwaves and UV radiation using an immersed source without the need of a microwave oven. The principles of functioning of the electrodeless source are given and discussed in terms of the experimental output UV energy, for applied microwave powers from 3 W to 60 W at 2450 MHz. This very efficient technical solution increases the control and yield, enabling the operator to work in safety conditions and using ordinary instruments and devices, also with metal parts, directly connected to the reactor. The method is versatile and the scale up for industrial applications is more feasible.

1. Introduction

It is well understood that the simultaneous application of microwave (MW) power and UV light leads to better results in photochemical processes [1–8]. The reactor is usually placed inside a commercial MW oven or in a waveguide applicator working at 2450 MHz, and the sample is submitted to UV radiation emitted by a mercury vapour lamp placed outside the oven. Higher yields are obtained in organic synthesis reactions [1], photo-initiated radical additions [2], the mineralization of water pollutants [3,7,8] and the removal of azo dyes, both in heterogeneous [4] and in homogeneous photocatalytic processes at a nearly constant temperature [5]. The possible effects of MW superheating in a Norrish type II reaction and in a photo-Fries reaction have also been discussed [7]. Despite these advantages, from a practical point of view commercial MW ovens have a number of drawbacks, the biggest being the lack of control of the MW power that actually acts on the sample. This may mean that it is difficult to gain deeper insight into the process and thus to achieve new results. In fact the specific absorption rate of MW power from each volume element of the sample, as a function of the time and of the position in the oven is very difficult, if not impossible, to predict. For the same reasons the spectral intensity of the light emitted by an immersed electrodeless MW/UV lamp like the one proposed by Církva and Hájek [2] to improve the efficiency of the MW/UV process, cannot be accurately controlled or measured. Moreover, the variations in temperature of a sample placed in the oven are difficult to control using a water bath. Metal probes or devices can be used only with caution and cumbersome auxiliary apparatus must be placed outside. Using an innovative and versatile method of MW assisted chemistry described in a previous paper [9], we built a fully integrated MW/UV photochemical reactor, which is easy to handle and performs well. In this paper we give details of the construction of the integrated reactor, plus the results obtained in the oxidative decomposition of Acid Orange 7 (AO7) aqueous solutions applying in situ MW power, UV radiation and H_2O_2 (MW/UV/H_2O_2).

2. Materials and methods

2.1. Photoreactor

The photochemical reactor, as depicted in Fig. 1, was made entirely out of fused quartz. The coaxial electrodeless MW/UV lamp was constructed by sealing off a 15 mm external diameter quartz ML bulb, filled with about 1 mg Hg and 0.66 kPa of argon. A 5 mm × 3 mm fused quartz tubing T, coaxial to ML, was used to accommodate a coaxial dipole antenna, MA, operating at 2450 MHz and producing a plasma discharge inside the bulb. The point of maximum emission of MA, i.e. the feed point [9], is indicated with F. The dipole antenna was made out of a 2.5 mm semi-rigid coaxial cable (Microcoax, Pottstown, PA, USA, Mod. UT 100), with a maximum power handling capability of about 80 W. We attached the lamp

* Corresponding author. Tel.: +39 050 315 2245; fax: +39 050 315 2236.
E-mail address: ferrari@ipcf.cnr.it (C. Ferrari).

1010-6030/$ – see front matter © 2009 Elsevier B.V. All rights reserved.
doi:10.1016/j.jphotochem.2009.03.001

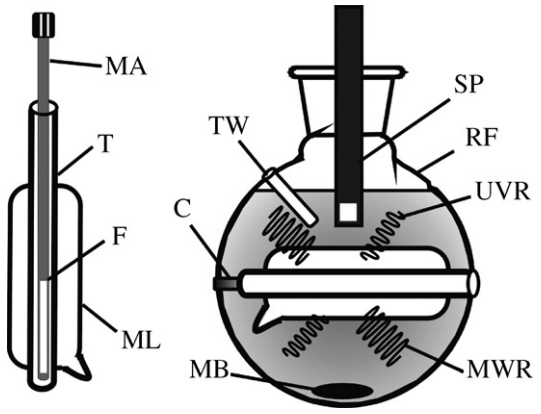

Fig. 1. The MW/UV quartz photoreactor. ML: bulb of the coaxial electrodeless UV lamp; T: quartz coaxial tubing; MA: microwave antenna; F: point of maximum MW power emission, or feed point; MB: magnetic stirring bar; RF: 100 ml quartz flask; SP: spectroscopic probe; TW: thermometric well; C: clamping post; MWR: radiated MW; UVR: UV light emission.

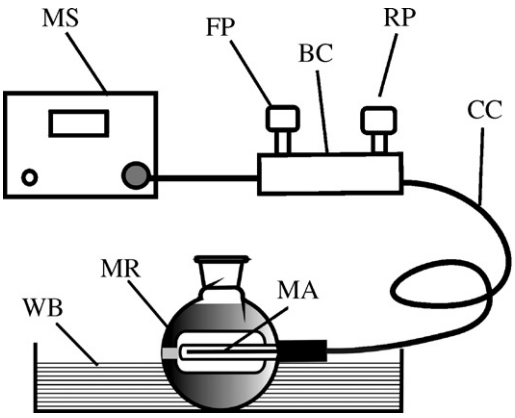

Fig. 2. Experimental setup. MS: 100 W, 2450 MHz, solid state source; BC: bi-directional coupler; FP: forward power probe-head; RP: reflected power probe-head; CC: flexible coaxial cable; MA: MW antenna; MR: microwave and UV reactor; WB: water bath.

to the inner wall of an ordinary 150 ml round RF flask, thus obtaining a very compact all-glass photochemical reactor. The dual source MW/UV could be used as an ordinary demountable device, working inside a glass or metal reactor of any shape, obtaining exactly the same results. The dual source was placed along a RF diameter, as shown in Fig. 1. The 5 mm tubing T was open at one end, while the other end was closed and sealed to the reactor wall using the clamping rod C to stiffen the device. A 2 mm inner diameter thermometric TW well was also applied, as depicted in Fig. 1. When the lamp was fed with a few tens W of MW power, start up was obtained touching the RF surface with the high voltage electrode of a laboratory vacuum leak detector (Tesla coil), or with the metal tip of a piezoelectric lighter (Sigma–Aldrich Mod. Z115231). In both cases the electrostatic field surrounding the charged point was sufficiently strong to accelerate some free electrons inside ML, initiating the plasma discharge. Interestingly, the dual source could emit only MW radiation (MWR) or both MW and UV radiation (MWR + UVR). To optimize the performance of the integrated reactor, F coincided with the centre of ML and of RF. The spectral ML emission and the absorbance of the aqueous dye solution from 200 nm to 1000 nm were recorded using the immersion 1/2 in. stainless steel probe SP (Avantes, Broomfield, CO, Mod. FDP-7UV200-2-VAS), connected to a fiberoptic spectrograph (Avantes, Broomfield, CO, Mod. Ava Spec 3648-UA-50-AF, not shown). The MW/UV source was only slightly perturbed by the presence of SP.

2.2. Setup

The MW apparatus is shown in Fig. 2. A magnetron source MS (Opthos, Knoxville, MD, Mod. MPG-4M), with a variable output power of up to 100 W in a continuous wave regime at 2450 MHz and provided with a coaxial 50 Ω output port, was used for the excitation of the lamp.

To measure the power applied P_{appl} to the microwave and UV reactor MR and the power reflected P_{refl} during the experiment, MS was connected to a coaxial 20 dB bi-directional coupler BC (Narda, Hauppauge, NY, Mod. 3022), using a MW power meter (Boonton, Parsippany, NJ, Mod. 4232A) and two power heads: FP (Mod. 51078) and RP (Mod. 51015), respectively, as shown in Fig. 2. Coupler BC was connected to MA using a calibrated flexible coaxial cable CC. More details of the microwave apparatus can be found in a precedent paper [9]. The temperature of the liquid inside the reactor was measured using a shielded type-K thermocouple sensor (Tersid, Milano, Mod. 55000) placed inside TW. A magnetic stirrer (not shown) was used to equilibrate the temperature and to mix the reactants with an ordinary stirring bar MB. In order to perform an isothermal process at room temperature the reactor was partially immersed in a flowing water bath WB, using cooled tap water from a thermostat and a double head peristaltic pump (not shown) so that the temperature of the reagents during the process was kept constant to within ±0.5 °C. We recorded the temperature of the reagents just at the lamp surface, T_1, and near the external wall of the reactor, T_2, using two 0.75 mm fiber-optic probes (FISO Technologies Inc., Saint-Foy, Quebec, Mod. FOT-M) with a thermometer (FISO Technologies Inc., Saint-Foy, Quebec, Mod. UMI4). The results showed that, when stirring and when the applied power was 20 W, the temperature difference was always $T_1 - T_2 < 0.5$ °C.

2.3. High-performance liquid chromatography (HPLC)

The degradation of AO7 was monitored by high-performance liquid chromatography using a P4000 (ThermoFinnigan) equipped with a Rheodyne 7125 injector (Rheodyne, Cotati, CA, USA), a 50 μl poly(etheretherketone) (PEEK tubing, Upchurch, Oak Harbor, WA) injection loop and an UV6000 diode array detector (ThermoFinnigan). Separations were carried out by a HyPurity C_{18} (Thermo Hypersil-Keystone, Thermo Finnigan Italia S.p.A, Milano, Italia) 250 mm × 4.6 mm RP column (silica particle size 5 μm). The column was eluted in isocratic mode with a mixture of 0.01% trifluoroacetic acid (TFA)–methanol 35:65 (v/v) with a flow rate of 0.7 ml/min. Detection was performed at 486 nm.

2.4. Reagents

All chemicals were of the highest available purity. Acid orange AO7 was obtained from Sigma–Aldrich. Hydrogen peroxide (30% m/m solution) and the double distilled water used for the aqueous solutions were obtained from Carlo Erba.

2.5. Sample preparation

The reactor was first washed with chromic and citric acids and thoroughly rinsed out with double distilled water. It was then filled with 120 ml of AO7 aqueous solution (typically $[AO7]_0 = 30$ mg/l), using H_2O_2 at various initial concentrations ($0 \le [H_2O_2]_0 \le 1660$ mg/l) to generate the active hydroxyl HO* radicals under the action of the UV radiation. Since the scope of this work was to present the advantages of using a novel experimental method of performing the oxidative decomposition of Acid Orange 7 azo dye by MW/UV/H_2O_2 process, we did not attempt to optimize the results. Accordingly, we did not use pH adjustments and all the

processes were carried out at nearly neutral values, $5 < pH < 7$, at atmospheric pressure and without gas bubbling inside MR.

3. Results and discussion

3.1. Source calibration

In Fig. 3A we show the intensities of the lines emitted by the MW electrodeless Hg lamp when MR was filled with double distilled water in thermal equilibrium at $T = 25.2 \pm 0.5\,^{\circ}C$, and $P_{appl} = 16.1 \pm 0.2$ W. The strong emission line of Hg vapours at 254 nm and the weaker Ar line at 811 nm are visible.

Fig. 3B shows the integrated spectral intensity of the 254 nm Hg line and of the 811 nm Ar line as a function of the temperature of the surrounding liquid, with $P_{appl} = 16.1 \pm 0.3$ W.

Fig. 3C shows the integrated intensity of the 254 nm and the 811 nm lines emitted by the lamp, as a function of P_{appl} when the temperature of the surrounding cooling water was $T = 26.8 \pm 0.5\,^{\circ}C$. The experiments demonstrated that the intensity of the 254 nm Hg line linearly increased when the temperature of the surrounding cooling water increased from 20 °C to 35 °C, while the intensity of the 811 nm Ar line decreased. Furthermore, the energy emitted by the two lines increased monotonically as a function of P_{appl}. As

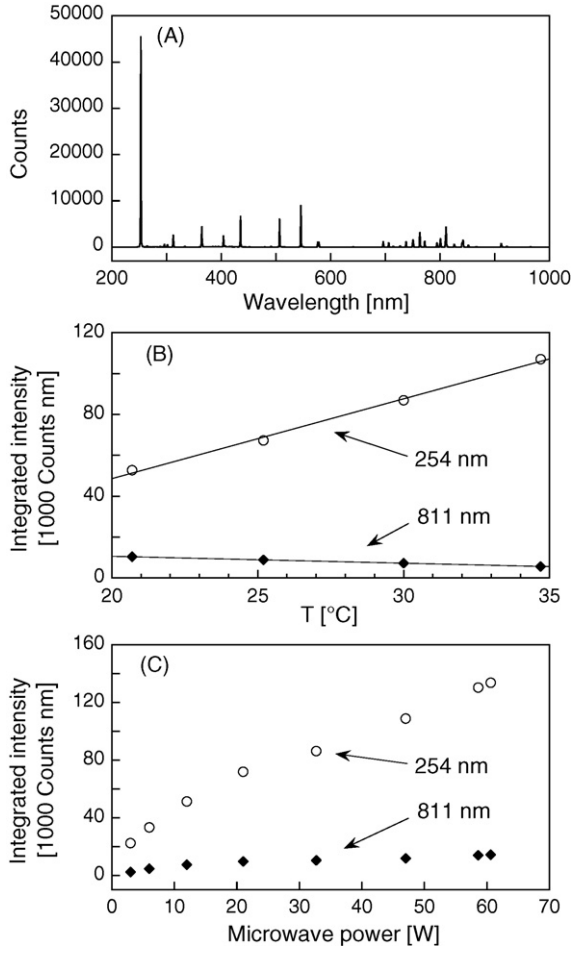

Fig. 3. (A) Spectral emission (Counts) of the Hg lamp immersed in double distilled water at $T = 25.2 \pm 0.5\,^{\circ}C$, in an interval of wavelengths from 200 nm to 1000 nm. $P_{appl} = 16.1 \pm 0.3$ W. (B) Integrated intensity of the 254 nm (open symbols) and 811 nm (full symbols) lines emitted by the lamp, when the reactor was fed with 16.1 ± 0.3 W as a function of the temperature of the surrounding cooling water, lines are linear fitting of the data. (C) Integrated intensity of the 254 nm (open symbols) and 811 nm (full symbols) lines, as a function of P_{appl}, when the temperature of the surrounding cooling water was $T = 26.8 \pm 0.5\,^{\circ}C$.

Fig. 3C shows, we were able to control the intensity of the UV line starting from $P_{appl} = 3$ W. Due to the wide-band characteristic of the coaxial dipole antenna MA we were able to feed the reactor with high efficiency without using any impedance matching device. In fact during the MW/UV process we obtained $P_{refl}/P_{appl} \leq 0.08$. A certified MW tester (Robin, Norwich, UK, Mod. TX 90) was used to measure any stray radiation escaping from the reactor during the experiments. When $P_{appl} = 20$ W and MR was filled with 120 ml of aqueous AO7 (30 mg/l) solution at $T = 23\,^{\circ}C$, the maximum density of radiated power measured over the entire external surface of MR was $P_{sr} = 0.85$ mW/cm^2. With S being the surface area of the reactor, $S \approx 120$ cm^2, the power P_{sr} $S \approx 102$ mW was lost (at maximum) and not used to activate the process. The small value of P_{sr} enabled us to work in complete safety, in agreement with International Commission on Non-Ionizing Radiation Protection (ICNIRP) guidelines. Actually, the ICNIRP reference level for occupational exposure to 2450 MHz electromagnetic radiation, measured at 5 cm from the surface of an MW apparatus, is $P_{sr} = 5$ mW/cm^2. The measures required when dealing with high MW powers in a glass reactor are described elsewhere [9]. Using the MW tester we verified that MA had the $\sin^2\theta$ radiation–intensity power pattern typical of a short dipole antenna, θ being the angle that the radius vector at F (see Fig. 1) makes with the MA axis [10]. The MW power absorbed by the plasma in the lamp per unit applied power, i.e. the lamp radiation efficiency, was: $\eta = 0.23 \pm 0.05$ W/W. This was calculated using the formula: $\eta = 1 - P_{irr}/(P_{appl} - P_{refl})$, where P_{irr}, obtained by numerical integration, was the overall MW power emitted by the lamp, in the absence of water. The efficiency η could be varied, within limits, by a suitable choice of the geometry and filling pressure.

In order to better understand the energy balance of the process occurring in the photochemical reactor, we estimated the percentage of microwave power effectively delivered to the liquid sample through the measurement of the temperature gradient in adiabatic conditions and in presence of the stirrer. In this calorimetric method the temperature increase, ΔT, of 80 ml deionized water was recorded during a short time interval, Δt, using the FISO fiber-optic thermometer, when the lamp was off. The same record was repeated when the lamp was switched on. Indicating with P_{del} the MW power effectively delivered to the lamp in each case, $P_{del} = P_{appl} - P_{refl}$ and using the formula $\Delta T/\Delta t = P_{del}/\Sigma_i m_i c_i$, where c_i and m_i were the specific heat and mass of each reactor component, we obtained $\eta \sim 0.20 \pm 0.05$. In the calorimetric experiments we applied a MW power of about 20 W and the temperature rise in water was recorded during time intervals in the range $10\,s < \Delta t < 30\,s$. This result was consistent with the more precise determination of η obtained when the lamp was working in air.

The MW power not absorbed by the lamp, MWR in Fig. 1, was available for the thermal activation of the reaction. When the reflected power was small ($P_{refl} \ll P_{appl}$), the power absorbed by the lamp, mostly converted in UV radiation as Fig. 3A shows, was given by $P_{lamp} = \eta P_{appl}$. An investigation of the radio-electric characteristics of the new light source is ongoing and the results will be provided in another paper. We will not discuss about non-thermal effects of MW radiation.

3.2. The decoloration process with H_2O_2

Immediately after the lamp was switched on, we continuously recorded the variations in absorbance and in temperature of the stirred AO7 aqueous solution. In Fig. 4 we show the spectral absorbance of the AO7 solution, with an initial concentration of $[AO7]_0 = 30$ mg/l and at temperature $T = 25.5 \pm 0.5\,^{\circ}C$, recorded at different times during the action of the MW/UV source, without the need of periodic sample withdrawals. In this experiment $P_{appl} = 17.2 \pm 0.3$ W and initial concentration $[H_2O_2]_0 = 308$ mg/l.

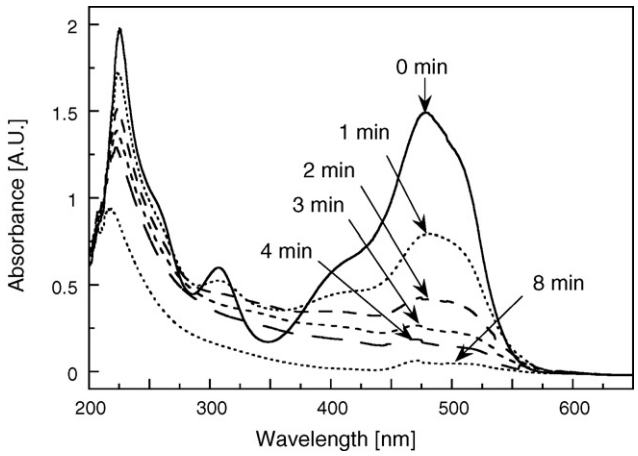

Fig. 4. Absorbance of AO7 solution at $T = 25.5 \pm 0.5\,^{\circ}C$ under the action of MW/UV/H_2O_2. The reactor was fed with 17.2 ± 0.3 W of MW power and $[H_2O_2]_0 = 308$ mg/l.

In Fig. 5A the semi-logarithmic plot of the absorbance at 483 nm, when $P_{appl} = 17$ W is reported as a function of time at various initial hydrogen peroxide concentrations.

The rate constant, $k_{1,483}$ obtained in the decoloration processes performed at constant temperature was calculated assuming a pseudo-first order reaction and utilizing the absorbance of the solution at the characteristic chromophore wavelength $\lambda = 483$ nm. The deviation from the first-order behaviour is discussed in Section 3.4. The rate constant values obtained from the data of Fig. 5A are reported in Fig. 5B as a function of $[H_2O_2]_0$. The rate constant shows a maximum value for the 308 mg/l $[H_2O_2]_0$ concentration and, caused by the recombination of radical species, a decrease at higher $[H_2O_2]_0$ values.

We ascertained that the presence of the stainless steel probe SP had no influence on the kinetics of the process. To this end we measured the rate constant of the reaction, $k_{1,483}$, under the action of MW/UV with and without the metal probe obtaining exactly the same result, within possible experimental errors.

Chemistry of UV/H_2O_2 photodegradation—MW assisted of model aromatic compounds has been well elucidated by Klan et al. [11,12]. Degradation usually relies on the generation of OH* radicals formed by means of the O–O bond cleavage ($H_2O_2 + h\nu \rightarrow 2OH^*$) and the following propagation and termination steps. The molar absorptivity of hydrogen peroxide is low above 250 nm, and two OH* radicals are formed per incident 254 nm photon absorbed in liquid aqueous solutions [13].

These radicals react rapidly and non-selectively with aromatic molecules primarily by addition–elimination reactions to form the corresponding hydroxyl compounds, or by hydrogen abstraction. Hydrocarbons are, e.g., oxidized by hydrogen abstraction to alcohols or carbonyl compounds or carboxylic acids [12].

A schematic degradation pathway of AO7 by OH* radicals can be proposed, based on the well-assessed mechanism proposed for other aromatic molecules [11,12]. The oxidative degradation of AO7 likely occurs in three stages and starts with the breaking of the azo bond, the most active group in the structure [14], to form 4-aminobenzenesulphonic acid and 1,2-naphthalenediolo. The second stage includes the hydroxylation of 4-aminobenzenesulphonic acid to hydroxylated or polyhydroxylated derivatives, which are oxidized in their turn to quinoid structures, and of 1,2-naphthalenediolo to 2-hydroxy- and 2,3-dihydroxy-1,4-naphthalenedione. As polyhydroxylated and quinoid structures are unstable, they lead to the formation of short-chain carboxylic acids by oxidative ring opening reactions. The third stage involves the oxidation of the formed carboxylic acids to CO_2.

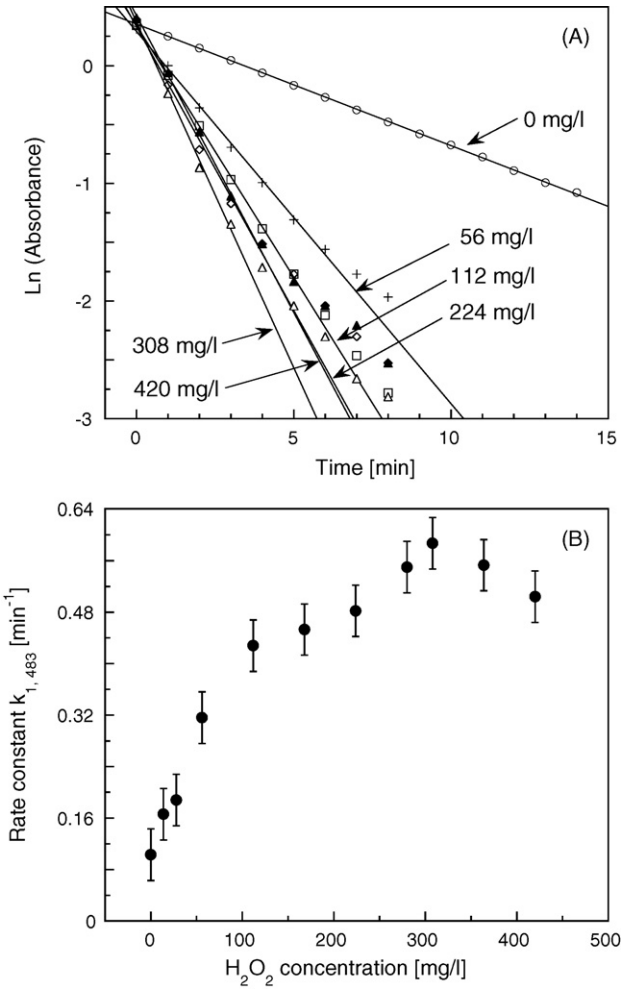

Fig. 5. (A) Semi-logarithmic plot of the absorbance of AO7 solution (30 mg/l) at 483 nm vs. time at various initial H_2O_2 concentrations, with $P_{appl} = 17 \pm 0.3$ W and $T \sim 25\,^{\circ}C$ (open circle: 0 mg/l, cross: 56 mg/l, open square: 112 mg/l, open diamond: 224 mg/l, open triangle: 308 mg/l, full triangle: 420 mg/l), lines are the linear fitting to the ln(absorbance) data larger than −1.5. (B) Rate constant $k_{1,483}$ (min^{-1}) of decoloration of AO7 aqueous solution (30 mg/l) as a function of $[H_2O_2]_0$, with $P_{appl} = 17 \pm 0.3$ W and $T \sim 25\,^{\circ}C$, obtained from data of panel (A).

3.3. The decoloration process without H_2O_2

The efficiency of our method in terms of reduction of chemical consumption was confirmed by the results obtained in the absence of hydrogen peroxide ($[H_2O_2]_0 = 0$) and reported in Fig. 6A. In this experiment $P_{appl} = 34.8 \pm 0.3$ W and $P_{lamp} = 7.8 \pm 0.3$ W.

Fig. 6B shows the semi-logarithmic plots of the absorbance of AO7 solution (30 mg/l) at 483 nm in a process performed at room temperature without hydrogen peroxide, at various MW powers.

Analysing the data reported in Fig. 6B, we concluded that the reactions performed by applying a MW power of 16 W, 34.8 W and 47.45 W were of the first order during the first stage of the reaction. The rate constants resulted: $k_{1,483} = 0.10$ (min^{-1}), $k_{1,483} = 0.17$ (min^{-1}) and $k_{1,483} = 0.23$ (min^{-1}), respectively. Also in this case we ascertained that the presence of the stainless steel probe SP had no influence on the kinetics of the process. The $k_{1,483}$ values were substantially higher than the ones obtained by other authors studying AO7 removal in contaminated water by photo oxidation processes with UV and $[H_2O_2]_0 = 0$. A possible explanation is that the in situ MW/UV source is capable of producing reactive HO* radicals directly in the AO7 aqueous solution with $[H_2O_2]_0 = 0$. This result is of interest, since, as it is well understood, the concentra-

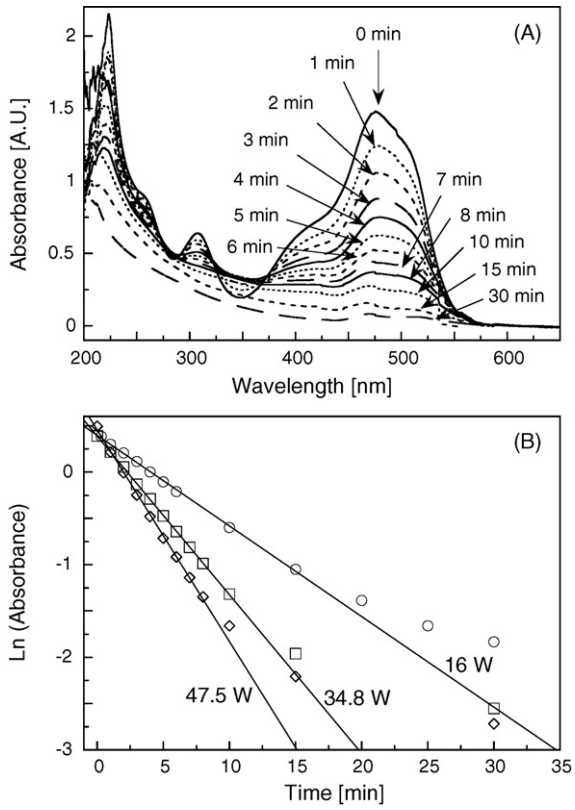

Fig. 6. (A) Absorbance of AO7 solution (30 mg/l) during the decoloration process obtained in the absence of H_2O_2. The power at the reactor's input was $P_{appl} = 34.8 \pm 0.3$ W, the power absorbed by the lamp was $P_{lamp} = 7.8 \pm 0.3$ W and $T = 25.0 \pm 0.5$ °C. (B) Semi-logarithmic plots of the absorbance of AO7 solution (30 mg/l) at 483 nm vs. time, at room temperature, in a process without hydrogen peroxide at various applied powers (open circle 16 ± 0.3 W, open square 34.8 ± 0.3 W, open diamond 47.5 ± 0.3 W), lines are the linear fitting to the ln(absorbance) data larger than −1.5.

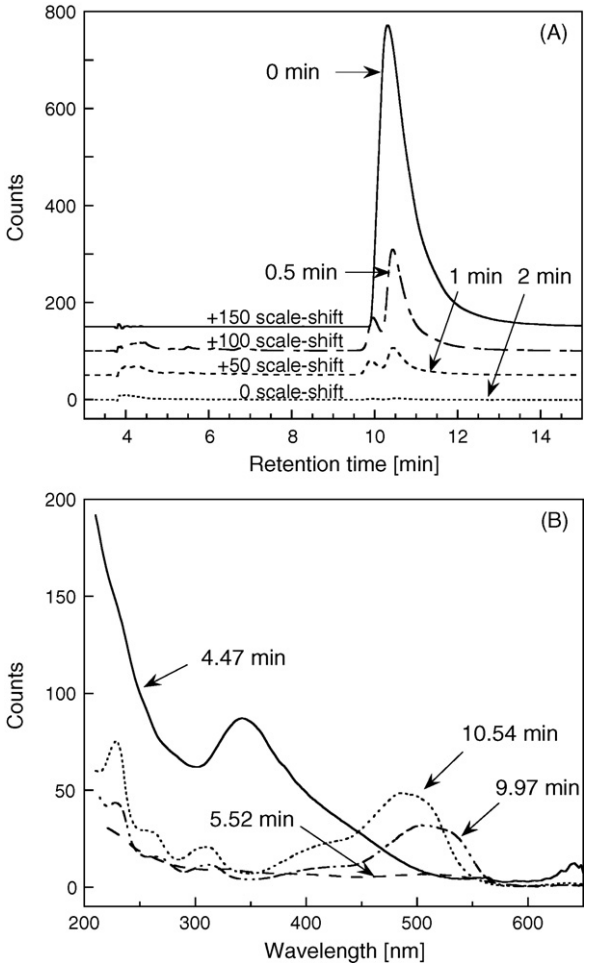

Fig. 7. (A) Absorbance chromatograms at 486 nm of 30 mg/ml AO7 under the action of MW/UV/H_2O_2 at different times, as indicated. The reactor was fed with 25.0 ± 0.3 W of MW power, $[H_2O_2]_0 = 308$ mg/l and $T = 25$ °C. Curves are shifted for clarity, as indicated. (B) The absorption spectra of the chemical products extracted at different retention time, as indicated, after 1 min of action of MW/UV/H_2O_2.

tion $[H_2O_2]_0$ is crucial for the degradation rate. For instance, in a recent work of Daneshvar et al. [15], the photo oxidation process with $[AO7]_0 = 20$ ppm performed using a commercial 30 W UV-C lamp was nearly completed in 12 min when $[H_2O_2]_0 = 5$ mmol/l, but when $[H_2O_2]_0 = 0$ the removal efficiency of AO7 decreased nearly to zero.

3.4. Deviation from the first-order behaviour

The experimental data in Figs. 5A and 6B fit well with the straight lines during the early stage of the reaction, indicating that the decoloration process performed with and without H_2O_2 are a pseudo-first order reaction. Deviation from the linear behaviour occurs in the late stage of the reaction, at low AO7 concentration, when the ln(absorbance) is about −1.5 A.U. The deviation occurs almost independently of the $[H_2O_2]_0$ value and of the MW power applied.

The deviation is the result of contribution of specific and aspecific UV/vis absorptions at about 486 nm of aromatic intermediates and short-chain carboxylic acids, as is demonstrated by HPLC analysis. This contribution is considerable when the AO7 concentration decreases and the by-products concentration increases. Fig. 7A shows absorbance chromatograms at 486 nm of 30 mg/ml AO7 before and after treatment with MW/UV/H_2O_2 at different times (0 min, 0.5 min, 1 min and 2 min). Fig. 7B shows the UV/vis spectra corresponding to four peaks of chromatogram (reaction time = 1 min) at retention time $t_R = 4.47$ min, 5.52 min, 9.97 min and 10.54 min.

The peak at 10.54 min was assigned to AO7. Its UV/vis spectrum is analogous to that reported in Figs. 4 and 6A ($t = 1$ min). As the photochemical degradation of AO7 occurs, HPLC analysis of reaction products shows a decrease of AO7 peak and the appearance of less idrophobic peaks. The peak at $t_R = 9.97$ min, not baseline separated from AO7, may correspond to aromatic, hydroxylated intermediates of AO7. Their UV spectrum shows a significant red shift of the λ_{max} from 488 nm to 506 nm (Fig. 7B), compatible with the loss of 4-aminobenzensulphonic acid and conjugation of OH and C=O group electrons with the aromatic ring. Not resolved peaks between $t_R = 4$ and 7 min likely correspond to short-chain carboxylic acids and aromatic compounds [16]. The peak at $t_R = 4.47$ min exhibits, for example, a big absorption at 347 nm, typical of aromatic conjugate compounds; the peak at $t_R = 5.52$ min has a spectrum similar to AO7 by-products after 8 min of treatment (Fig. 4).

3.5. Comparison with other methods of decoloration of AO7 with UV/H_2O_2

The results of our reactions, each performed in triplicate, are summarized in Table 1, reporting the initial concentrations of AO7 (column 2) and of H_2O_2 (column 4). The MW applied power (column 3) and the reaction temperature (column 5) are also indicated.

Table 1
Pseudo-first order rate constants for decoloration of AO7 by MW/UV/H_2O_2 at different initial concentrations of AO7, of H_2O_2 and at various applied powers.

No.	$[AO7]_0$ (mg/l)	MW applied power P_{appl} (W) ± 0.3 (W)	$[H_2O_2]_0$ (mg/l)	Temperature (°C) ± 0.5 (°C)	Rate constant $k_{1,483}$ (min^{-1}) ± 0.01 (min^{-1})
1	30	17.0	0	25.0	0.10
2	30	16.8	14	25.1	0.17
3	30	16.7	28	25.3	0.19
4	30	17.1	56	25.6	0.34
5	30	17.0	112	24.8	0.43
6	30	16.6	168	25.2	0.50
7	30	16.7	224	25.5	0.56
8	30	17.1	280	25.5	0.59
9	30	17.2	308	25.5	0.65
10	30	16.7	364	25.2	0.59
11	30	16.9	420	25.2	0.49
12	30	16.0	0	23.0	0.10
13	30	34.8	0	25.0	0.17
14	30	47.5	0	24.6	0.23
15	30	30.0	0	22.0	0.12
16	17	53 ($W l^{-1}$)	1660	25.6	1.00
17	100	40	408	38.0	0.28

Table 2
Pseudo-first order rate constants for decoloration of AO7, $k_{1,483}$, obtained by other authors with UV/H_2O_2.

No.	$[AO7]_0$ (mg/l)	Applied power P_{appl} (W)	$[H_2O_2]_0$ (mg/l)	Temperature (°C)	Rate constant $k_{1,483}$ (min^{-1})	Reference
18	30	30	80	22 ± 2	0.105	[19]
19	17	83.33 $W l^{-1}$	1662	25.6	0.73	[20]
20	100	700 (MW oven) + 28.1 (UV lamp)	408	38 ± 1	0.16	[21]
21	31.5	15	680	Room	0.17	[22]

The power applied to the reactor in reaction No. 16 is given in terms of light intensity per unit volume of solution and will be used in the following as a comparison. We found that the degradation of AO7 by hydrogen peroxide was negligible in the absence of UVR.

Studies on the decoloration processes of azo dyes have been carried out by other authors using various procedures [17–22]. Reactions reported in Table 2 were performed by various laboratories to obtain the decoloration of AO7 with MW/UV/H_2O_2 using a commercial microwave system [21], or with UV/H_2O_2 using a commercial Hg lamp [19,22], also varying the gap size [20].

We compared reactions No. 18, No. 19, No. 20 and No. 21 in Table 2, performed by other authors [19–22], and reactions No. 15, No. 16, No. 17 and No. 2 in Table 1, respectively, performed with our method in similar experimental conditions, as far as chemical concentration, applied power and reaction temperature were of concern. The results are summarized in Table 3.

Inspection of data in Table 3 reveals that the novel microwave photoreactor was always useful to save time and/or energy and/or chemicals in the oxidative decomposition of Acid Orange 7 azo dye using MW/UV/H_2O_2 process. Furthermore, we were able to accurately measure the power applied and absorbed by the sample, safely working in fairly better experimental conditions. Making reference to reaction No. 20 it is worth noting that the authors, attempting to estimate the maximum MW power absorbed by the lamp in the MW oven, admitted the impossibility of performing a direct measurement [21]. This inconvenient depends on the principle of functioning of the MW oven. It is well known that in a multimode resonant cavity the local density of electromagnetic energy strongly depends on the geometry, position and permittivity of the sample, so that the MW power absorbed by the reagents and the intensity of the UV radiation emitted by the lamp are hardly predictable or controllable during the activation process.

Table 3
Advantages obtained using the present method in decomposition of Acid Orange 7 azo dye in water solution, with the same initial concentration $[AO7]_0$, by MW/UV/H_2O_2 process.

Reactions in comparison	Rate constant $k_{1,483}$ (min^{-1})	$[H_2O_2]_0$ (mg/l)	Power (W)
15 (this work) and 18 [19]	0.12 vs. 0.105	0 vs. 80	idem
16 (this work) and 19 [20]	1.00 vs. 0.73	idem	53 ($W l^{-1}$) vs. 83.33 ($W l^{-1}$)
17 (this work) and 20 [21]	0.28 vs. 0.16	idem	idem
2 (this work) and 21 [22]	idem	14 vs. 680	idem

3.6. Scale up

The high activation efficiency and the possibility of utilizing auxiliary instruments, also cumbersome and with metal part, directly connected to the reactor, make the method very useful for research work. Moreover, the possibility of in situ applying high MW and UV powers using a number of dual sources makes the method a good candidate to substitute the trickier and more expensive applicators based on a closed multimode resonant MW cavity [1–8]. The method of thermal activation using an array of independent (non-interfering) microwave coaxial applicators has been recently presented [23]. The preliminary experiments demonstrated that a few kW of MW power can be applied by simply increasing the number of the applicators. A highly reproducible heating pattern is obtainable, also working in a metal vessel, with a MW installable power of the order of 350 W per inch of reactor length at 2450 MHz and at working temperatures up to 800 °C using SiO_2 coaxial cable for the construction of the feeding MW antenna. The method opens the way of breaking the scale up barrier for industrial applications. Interestingly, the use of a suitable number of independent MW/UV sources, as depicted in Fig. 8, enables the scale up also for processes of MW assisted photochemistry. The H_2O_2 is added to the AO7 aqueous solution at the input IN of the continuous flow photoreactor R and the reagents, being submitted to MW and UV radiations, reach the output port OUT to be reused or discharged.

Each one of the MW/UV sources immersed in the liquid continuously flowing in the (metal) reactor R can be fed with a known amount of MW power, tailored as a function of $[AO7]_0$, of $[H_2O_2]_0$ and of the requested throughput. Actually the coaxial electrodeless lamp, not yet commercially available, can be constructed using ordinary laboratory equipments (glass works and vacuum system).

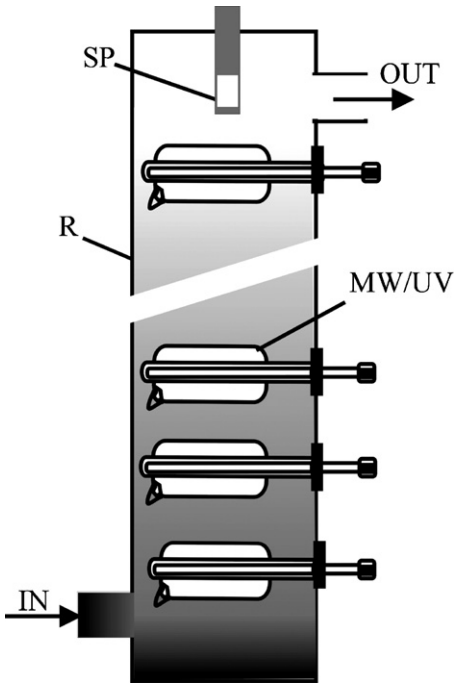

Fig. 8. Scheme of a continuous flow photoreactor working with a number of in situ MW/UV sources. R: metal walled reactor; MW/UV: integrated source; SP: spectroscopic immersed sensor; IN/OUT: input/output ports.

C.N.R. patent is pending. The use of ordinary probes (like thermocouples) enables standard process control methods. This scheme is highly flexible and greatly reduces the project work.

4. Conclusions

The microwave photochemical reactor utilized in this work for the oxidative decomposition of Acid Orange 7 azo dye by MW/UV/H_2O_2 process enabled to measure and control the MW power, leading to a greater and more realistic knowledge of the energetic aspects of a process, which as far as we know has not been possible before with this degree of accuracy. From a general point of view, the use of a dual source placed inside the reagents was in itself mostly efficient, especially if synergetic effects are important [1–8]. In fact, in this experimental configuration, the MW available power was completely utilised to produce UV radiation and volumetric heating, both contributing to the decoloration process, with no energy loss to the ambient or to the walls of an oven. The possibility of recording the spectroscopic data during the process without the need for periodic sample withdrawals and using ordinary auxiliary techniques were additional advantages. Working on the bench without needing an oven we obtained a substantial reduction in the time spent in preparing and performing each reaction, saving time and chemicals in the oxidative decomposition of Acid Orange 7. Compared to other MW commercial equipments currently in use [8,17,18,21] our method is more versatile and useful for the construction of MW/UV photo reactors of industrial interest.

Acknowledgements

The authors would like to thank the Italian National Research Council, CNR, for the financial support of this work. This work has been undertaken as a part of the I.P.C.F. Research Project: Development of Microwave Techniques for Civil and Industrial Applications.

References

[1] S. Chemat, A. Aouabed, P.V. Bartels, D.C. Esveld, F. Chemat, J. Microwave Power Electromagn. Energy 34 (1998) 55–60.
[2] V. Církva, M. Hájek, J. Photochem. Photobiol. A: Chem. 123 (1999) 21–23.
[3] S. Horikoshi, A. Tokunaga, N. Watanabe, H. Hidaka, N. Serpone, J. Photochem. Photobiol. A: Chem. 177 (2006) 129–143.
[4] S. Horikoshi, H. Huiaka, N. Serpone, Environ. Sci. Technol. 36 (2002) 1357–1365.
[5] C. Galindo, A. Kalt, Dyes Pigments 42 (1999) 199–207.
[6] Z. Ai, P. Yang, X. Lu, J. Hazard. Mater. B 124 (2005) 147–152.
[7] P. Klan, J. Literak, S. Relich, J. Photochem. Photobiol. A: Chem. 143 (2001) 49–57.
[8] D.H. Han, S.Y. Cha, H.Y. Yang, Water Res. 38 (2004) 2782–2790.
[9] I. Longo, A.S. Ricci, J. Microwave Power Electromagn. Energy 41 (2007) 1–16.
[10] J.D. Kraus, R.J. Marhefka, Antennas, McGraw Hill, New York, 2002.
[11] P. Klan, M. Vavrik, J. Photochem. Photobiol. A: Chem. 177 (2006) 24–33.
[12] J. Dolinova, R. Ruzicka, R. Kurkova, J. Klanova, P. Klan, Environ. Sci. Technol. 40 (2006) 7668–7674.
[13] J.P. Hunt, H. Taube, J. Am. Chem. Soc. 74 (1952) 5999–6002.
[14] J. Bandara, C. Morrison, J. Kiwi, C. Pulgarin, P. Peringer, J. Photochem. Photobiol. A: Chem. 99 (1) (1996) 57–66.
[15] N. Daneshvar, S. Aber, F. Hosseinzadeh, Global NEST J. 10 (2008) 16–23.
[16] R.M. Silverstein, G.C. Bassler, T.C. Morril, Spectrometric Identification of Organic Compounds, IV edition, John Wiley & Sons, New York, 1981, pp. 308–329.
[17] P. Klan, M. Hajek, V. Církva, J. Photochem. Photobiol. A: Chem. 140 (2001) 185–189.
[18] S. Horikoshi, H. Hidaka, N. Serpone, Environ. Sci. Technol. 36 (2002) 5229–5237.
[19] M.A. Benhnajady, N. Modirshahla, M. Shokri, Chemosphere 55 (2004) 129–134.
[20] A. Azam, A. Hamid, J. Hazard. Mater. B 133 (2006) 167–171.
[21] X. Zhang, G. Wang Ym Li, J. Qu, J. Hazard. Mater. B 134 (2006) 183–189.
[22] A. Aleboyeh, Y. Moussa, K. Aleboyeh, Sep. Purif. Technol. 43 (2005) 143–148.
[23] I. Longo, A.S. Ricci, L. Gasperini, in: S. Lupi (Ed.), Book Of Abstracts, HES-07 International Symposium on Heating by Electromagnetic Sources, Padua, Italy, pp. 227–231, 2007.